

# Design of low-threshold compact Au-nanoparticle lasers

X. F. Li<sup>1,\*</sup> and S. F. Yu<sup>2,3</sup>

<sup>1</sup>*School of Electrical and Electronic Engineering, Nanyang Technological University, Singapore 639798, Singapore*

<sup>2</sup>*Present address: Department of Applied Physics, Hong Kong Polytechnic University, Hung Hom, Kowloon, Hong Kong*

<sup>3</sup>*e-mail: sfyu21@hotmail.com*

*\*Corresponding author: xfl\_79@yahoo.com.cn*

Received February 12, 2010; accepted June 27, 2010;  
posted July 7, 2010 (Doc. ID 124096); published July 21, 2010

We performed a rigorous study to reduce threshold gain of Au-nanoparticle lasers in the deep-subwavelength scale with the consideration of strong interband transitions in Au and device dimensions. We found that the high-threshold optical gain of the nanolaser (over  $10^5 \text{ cm}^{-1}$ , which is matched with the result estimated from a previous article [Nature **460**, 1110 (2009)]) arises from the high interband transition of Au near 530 nm. It can be shown that by increasing the background index, as well as optimizing the lasing wavelength and device dimensions, the threshold gain (cavity volume) can be reduced by 43% (90%). © 2010 Optical Society of America

OCIS codes: 240.6680, 140.3460, 290.5850.

Nanoparticle lasers (NPLs) in the deep-subwavelength dimension are extremely useful in high-density storage, lithography, sensing, and medical applications [1–4]. However, it is a challenge in experiments to observe lasing from this type of lasers due to their high cavity loss. Recently, Noginov *et al.* reported coherent lasing action at  $\sim 530 \text{ nm}$  from a nanoparticle array, which was made by Au nanoparticles surrounded with thin layers of active dye polymer, with an average cavity size of  $\sim 44 \text{ nm}$  [5]. This work led to extensive attention on supercompact nanolasers [6,7]. However, the required optical gain to achieve lasing from such a nanosize cavity is extremely high (on the order of  $10^5 \text{ cm}^{-1}$ ), especially when Au is used [8], which increases the fabrication complexity and hinders the applications of this type of lasers. Our question is, can we further reduce either the cavity size or the threshold gain of the NPLs?

It is necessary to perform a systematic investigation to find a way to design a NPL with an affordable threshold gain. Previously, a metal core embedded inside an infinitely thick gain medium was adopted as the most simplified model to analyze the lasing characteristics of NPLs [9,10]. However, the gain region cannot be infinitely thick, and the size dependence of the metal permittivity must be taken into account in the study of the nanodevices. In this Letter, a more realistic configuration is considered and the corresponding singular condition is derived in order to find a way to minimize the threshold gain of the NPLs. The low-loss lasing wavelengths and several designs under the required threshold criteria will be proposed. Results show that both the lasing threshold and cavity size of the NPLs can be further reduced.

Figure 1(a) shows the schematic of an Au-NPLs with the gain medium uniformly distributed over the region of  $R_M \leq r \leq R_G$ . To model the laser accurately, the exact metal permittivity exhibiting strong dependence on wavelength and device dimension should be used. Hence, a modified Drude formula, with the consideration of the interband transitions, is used [11]:

$$\varepsilon_M = \varepsilon_\infty - \frac{\omega_p^2}{\omega^2 + i\gamma\omega} + \varepsilon_{x1} + \varepsilon_{x2}, \quad (1)$$

where  $\varepsilon_\infty$  is the permittivity under the high-frequency limit,  $\omega_p$  is the bulk plasma frequency, and  $\gamma$  is the electron decaying rate. If the metal nanoparticle has a size equivalent to the bulk mean-free path length of the conduction electrons,  $\varepsilon_M$  will exhibit a strong dependence on its dimension. This can be included into the decaying rate  $\gamma = \gamma_\infty + V_F/R_M$ , where  $\gamma_\infty$  is the bulk value and  $V_F (= 1.39 \times 10^6 \text{ m/s})$  is the Fermi velocity [10]. It should be noted that the quantum effects can be discarded, even though  $R_M$  is 7 nm due to the extremely high conduction electron concentration ( $\sim 10^{23} \text{ cm}^{-3}$ ) in the metal. Our treatment will be invalid if  $R_M \leq 1 \text{ nm}$ . This is because the amount of energy obtained by the individual electron per

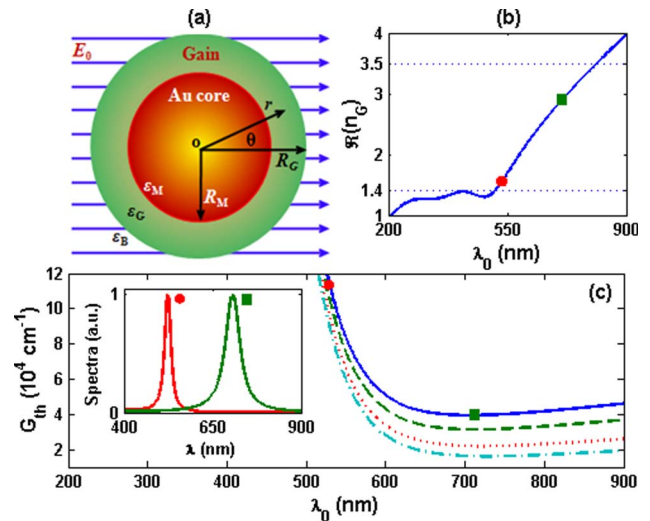


Fig. 1. (Color online) (a) Schematic of an NPL composed of an Au core (with radius  $R_M$  and permittivity  $\varepsilon_M$ ), an active region (with radius  $R_G$  and permittivity  $\varepsilon_G$ ), and an infinite background dielectric (with permittivity  $\varepsilon_B$ ). The static electric field has the amplitude of  $E_0$  and wavelength of  $\lambda$ . Plots of (b)  $\Re(n_G)$  and (c)  $G_{th}$  versus lasing wavelength  $\lambda_0$  (fulfilling the singular condition) for different values of  $R_M$  [i.e., 7 nm (solid curve), 10 nm (dashed curve), 20 nm (dotted curve), and 50 nm (dashed-dotted curve)]. The inset of Fig. 1(c) shows the lasing spectra with  $n_G = 1.516 - 0.473i$  as indicated by  $\bullet$  [ $\lambda_0 = 524 \text{ nm}$ ] and  $n_G = 2.884 - 0.223i$  as indicated by  $\blacksquare$  ( $\lambda_0 = 710 \text{ nm}$ ) to obtain the lowest  $G_{th}$ .

incident photon excitation becomes comparable with  $k_B T$  ( $k_B$ , Boltzmann constant;  $T$ , absolute temperature) [4].

In previous studies, the laser was assumed to be composed of a metallic core surrounded by a semi-infinite gain medium [9,10]. Here, we repeat the threshold calculation of this configuration with the consideration of interband transitions of Au. It has a singular condition of a simple form:  $\epsilon_M + 2\epsilon_G = 0$ , where  $\epsilon_G (= n_G^2)$ . Based on this expression and Eq. (1), the required refractive index of the gain medium,  $\Re(n_G)$ , and threshold gain,  $G_{th} [= -4\pi \times I(n_G)/\lambda_0$ , where  $\Re(n_G)$  and  $I(n_G)$  denote the real and imaginary parts of  $n_G$ , respectively] [12], to achieve singularity of field intensity can be calculated. Figures 1(b) and 1(c) plot  $\Re(n_G)$  [ $G_{th}$ ] versus resonant wavelength,  $\lambda_0$ , under different  $R_M$  choices. It is observed that the value of  $G_{th}$  increases exponentially if  $\lambda_0 < 500$  nm. The interband transitions of Au led to a very strong metallic absorption ( $>3 \times 10^5$  cm $^{-1}$ ) at  $\lambda_0 \sim 400$  nm. Furthermore, the value of  $G_{th}$  increases rapidly with the reduction of  $R_M$ .

As  $\Re(n_G) \gg I(n_G)$ ,  $\Re(n_G)$  determines the resonant frequency of the laser. The range of  $\Re(n_G)$  should be set between 1.4 and 3.5 so that the allowed  $\lambda_0$  is varied between 510 and 820 nm [Fig. 1(b)]. If  $\Re(n_G) \sim 1.5$ , the value of  $\lambda_0$  should be around 530 nm [see • points in Fig. 1(c) and the lasing spectrum, inset], similar to that observed in experiments (e.g., see [5]). To achieve lasing, it is required that  $n_G = 1.516 - 0.473i$  and the corresponding  $G_{th} \sim 1.13 \times 10^5$  cm $^{-1}$  (which is  $\sim 5\%$  lower than the estimated value from [5], as  $R_G = \infty$  is used here). Such a stringent gain requirement makes it very difficult to realize lasing from Au-SiO $_2$  nanoparticles. A possible solution is to choose a wavelength far away from the interband region. Nevertheless, if  $\lambda_0$  is too large, the metallic loss will become extremely high. Therefore, there should be an optimal value for  $\lambda_0$  to achieve the lowest value of  $G_{th}$ . Figure 1(c) shows that the lowest absorption occurs at  $\lambda_0 \sim 710$  nm, which requires  $n_G = 2.884 - 0.223i$  [the lasing spectrum is inserted in Fig. 1(c); see ■]. In this case,  $G_{th}$  can be reduced by  $\sim 65\%$  (from  $1.13 \times 10^5$  to  $3.9 \times 10^4$  cm $^{-1}$ ).

Configuration of the above-mentioned NPLs may not be realistic, as  $R_G$  in practice cannot be extended infinitely. In the following paragraphs, a finite value of  $R_G$  and  $R_M = 7$  nm will be used. If  $R_G$  is finite, three layers will be formed and the modal singularity occurs when [13]

$$\frac{2(\epsilon_G - \epsilon_M)(\epsilon_G - \epsilon_A)}{(\epsilon_M + 2\epsilon_G)(\epsilon_G + 2\epsilon_A)} = \eta^3, \quad (2)$$

where  $\eta = R_G/R_M$ .

Figures 2(a) and 2(b) plot the variation of  $\Re(n_G)$  and  $G_{th}$ , respectively, versus  $\lambda_0$  and  $\eta$ . It is observed that the values of  $\Re(n_G)$  and  $G_{th}$  can be reduced with the increase of  $\eta$ . The variations of  $G_{th}$  versus  $\eta$  for three values of  $\lambda_0$  are plotted in Fig. 2(c). It is shown that for each  $\lambda_0$ , the laser threshold can be converged to a minimum value if  $\eta$  is large enough, due to the better coupling between the optical modes and the gain medium. As  $G_{th}$  is roughly inversely proportional to  $\eta$ , it is helpful to define a parameter  $\xi = |(G_{th} - G_{th0})/G_{th0}|$  to represent the amount of  $G_{th}$  deviating from its minimum value, i.e.,  $G_{th0}$  for a given value of  $\eta$ . Hence, the minimal value of  $\eta$  (i.e., the smallest

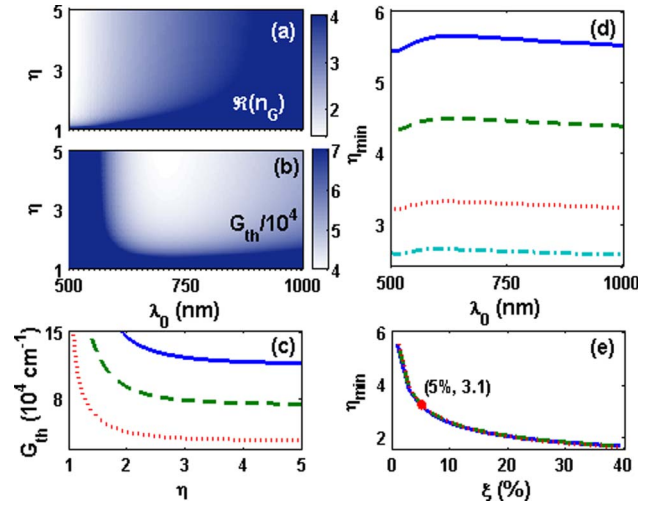


Fig. 2. (Color online) Images of (a)  $\Re(n_G)$  and (b)  $G_{th}$  in the plane of  $\lambda_0$  and  $\eta$ . (c) Plot of  $G_{th}$  versus  $\eta$  for different values of  $\lambda_0$  [530 nm (solid curve), 560 nm (dashed curve), and 710 nm (dotted curve)]. (d) Minimal  $\eta$  versus  $\lambda_0$  with different values of  $\xi$  [1% (solid curve), 2% (dashed curve), 5% (dotted curve), and 10% (dashed-dotted curve)]. (e) Minimal  $\eta$  versus  $\xi$  for different values of  $\lambda_0$  [530 nm (solid curve), 560 nm (dashed curve), and 710 nm (dotted curve)], where the value used in [5] is also indicated.

laser size) of the NPLs for a predetermined value of  $\xi$  can then be deduced. Figure 2(d) plots the minimal  $\eta$  versus  $\lambda_0$  for four predetermined  $\xi$  values. It is noted that for a NPL with  $\xi = 10\%$ ,  $R_G$  can be  $<2.5 \times R_M$ . However, if  $\xi = 1\%$ , the laser diameter (cavity volume) must be augmented by 2.33 (11) times. The detailed dependence of the minimal  $\eta$  upon  $\xi$  can be found in Fig. 2(e), where three lasing wavelengths have been considered. The plot shows a weak dependence of  $\lambda_0$ , while the minimal value of  $\eta$  increases exponentially with  $\xi$ . Besides, although the value of  $G_{th}$  varies with  $R_M$ , the minimal value of  $\eta$  is almost independent of  $R_M$ . It must be remembered that the value of  $\eta$  used in [5] is  $\sim 3.1$ , hence the corresponding value of  $\xi$  is 5%; see also Fig. 2(e). This is the reason why the value of  $G_{th}$  estimated from [5] for a finite gain NPL is different by 5% to that deduced from the infinite gain approximation (i.e.,  $\epsilon_M + 2\epsilon_G = 0$ ).

For NPLs with finite gain operating in an atmospheric environment, gain material with a high refractive index,  $\Re(n_G)$ , of  $\sim 2.88$  is required [14]. However, synthesis of high refractive index gain materials is more difficult than that of the dye-doped SiO $_2$  gain media [5]. Therefore, our question is whether it is possible to implement standard Au-SiO $_2$  NPLs with low threshold gain and cavity size. The answer is yes, because it can be done by increasing the refractive index of the background material,  $n_B$ .

In Figs. 3(a) and 3(b), the dependences of  $\Re(n_G)$  and  $G_{th}$  on  $n_B$  and  $\eta$  are depicted, where  $\lambda_0 = 710$  nm. As shown in Figs. 2(a) and 2(b), the values of  $\Re(n_G)$  and  $G_{th}$  are extremely large when  $\eta < 2$ ; these values, however, can be reduced significantly by setting  $n_B > 2.8$ . Figures 3(c) and 3(d) plot  $\Re(n_G)$  and  $G_{th}$ , respectively, versus  $n_B$  under different values of  $\eta$ . The control of  $n_B$  on the lasing characteristics is observed much more effectively for the small-size devices, while the values of  $\Re(n_G)$  and  $G_{th}$  are almost independent on  $n_B$  if  $\eta > 4$ . It

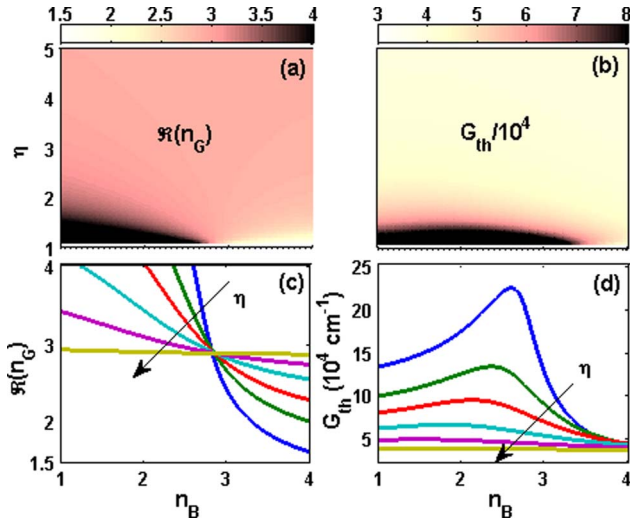


Fig. 3. (Color online) Images of (a)  $\mathcal{R}(n_G)$  and (b)  $G_{th}$  in the plane of  $n_B$  and  $\eta$ . Plots of (c)  $\mathcal{R}(n_G)$  and (d)  $G_{th}$  versus  $n_B$  for several values of  $\eta$  (i.e., 1.10, 1.18, 1.28, 1.48, 1.88, and 4.08, as indicated by arrows).  $\lambda_0 = 710$  nm is used in this calculation.

can be shown that the dependence of the resonant conditions of the NPLs on the value of  $n_B$  is achieved by adjusting the coupling strength of the optical field with the gain medium. Hence, if the active medium is too thick, the variation of  $n_B$  will hardly bring noticeable impact to the operation conditions of the NPLs.

Figure 4 replots Figs. 2(a) and 2(b) for the case of  $n_B = 3.25$ , where the parameters of the NPLs satisfied  $\mathcal{R}(n_G) \sim 1.4$  are marked by red dots. It is observed that small values of both  $\mathcal{R}(n_G)$  and  $G_{th}$  can be realized even with a small value of  $\eta$  (i.e., a very small laser size). It should be noted that the white region on the left side of the dots [see Fig. 4(a)] cannot be used to design an NPL, as the required  $\mathcal{R}(n_G)$  is too low to find an appropriate

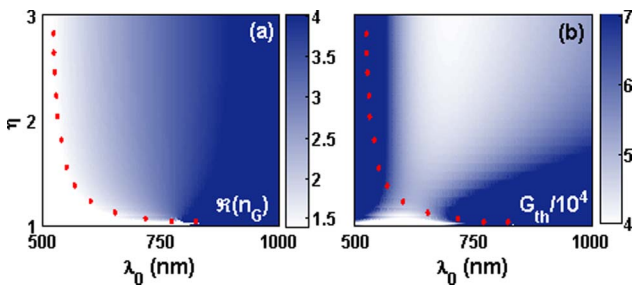


Fig. 4. (Color online) Images of (a)  $\mathcal{R}(n_G)$  and (b)  $G_{th}$  in the plane of  $\lambda_0$  and  $\eta$  with  $n_B = 3.25$  used in the calculation. In the figure, the positions where  $\mathcal{R}(n_G) \sim 1.4$  have been indicated by red dots.

host material. Using this design, the size and threshold gain of the NPLs can be reduced simultaneously. For example, a gold core with  $R_M = 7$  nm enclosed by a dye-doped  $\text{SiO}_2$  active medium with  $R_G = 10$  nm and  $n_G = 1.52$  can be embedded inside an ALAs background dielectric with  $n_B = 3.25$  to form an NPL with  $G_{th} \sim 6.4 \times 10^4 \text{ cm}^{-1}$  and  $\lambda_0 \sim 570$  nm (i.e., ALAs with negligible absorption). Using this configuration, the values of  $G_{th}$  and cavity volume can be reduced by 43% and 90%, respectively, when compared with that given in [5].

In conclusion,  $G_{th}$  of an Au NPL is calculated by examining the singularity of the supported modal field. Furthermore, the size dependence and interband transition of Au are taken into calculation. It is found that the extremely high value of  $G_{th}$  of the Au-particle nanolasers is due to the interband transition effect of Au at  $\lambda_0 = 530$  nm. However,  $G_{th}$  of the NPLs can be significantly reduced if (i) an appropriate value of  $\lambda_0$  is selected to avoid strong interband transition of Au, (ii) the condition  $n_B > \mathcal{R}(n_G)$  is used to improve the optical confinement of NPLs, and (iii) minimal laser size is chosen under the given threshold criterion. Results show that  $G_{th}$  (cavity volume) of the NPLs can be reduced by 43% (90%).

This work is supported by the A\*STAR (Agency for Science, Technology, and Research) SERC (Science and Engineering Council) under grant 082-101-0016.

## References and Notes

1. D. J. Bergman and M. I. Stockman, Phys. Rev. Lett. **90**, 027402 (2003).
2. H. A. Atwater, Sci. Am. **296**, 56 (2007).
3. N. M. Lawandy, Appl. Phys. Lett. **90**, 143104 (2007).
4. S. A. Maier, *Plasmonics: Fundamentals and Applications* (Springer, 2007).
5. M. A. Noginov, G. Zhu, A. M. Belgrave, R. Bakker, V. M. Shalaev, E. E. Narimanov, S. Stout, E. Herz, T. Suteewong, and U. Wiesner, Nature **460**, 1110 (2009).
6. F. J. Garcia-Vidal and E. Moreno, Nature **461**, 604 (2009).
7. J. Heber, Nature **461**, 720 (2009).
8. According to [5],  $2.7 \times 10^3$  dye molecules are distributed mainly in a region from  $r = 7$  to 12 nm, and the peak absorption cross section is estimated to be  $2.55 \times 10^{-16} \text{ cm}^2$ . The lasing threshold is then estimated to be  $G_{th} \sim 1.19 \times 10^5 \text{ cm}^{-1}$ .
9. N. M. Lawandy, Appl. Phys. Lett. **85**, 5040 (2004).
10. J. A. Gordon and R. W. Ziolkowski, Opt. Express **15**, 2622 (2007).
11. P. G. Etchegoin, E. C. Le Ru, and M. Meyer, J. Chem. Phys. **125**, 164705 (2006).
12. X. F. Li, S. F. Yu, and A. Kumar, Appl. Phys. Lett. **95**, 141114 (2009).
13. J. D. Jackson, *Classical Electrodynamics*, 3rd ed. (Academic, 1999).
14. L. M. Liz-Marzan, M. Giersig, and P. Mulvaney, Langmuir **12**, 4329 (1996).